

Structural Evolution of BaVS₃ Under Pressure

Alka B. Garg^a, Viswanathan Vijayakumar^a, Amitava Choudhury^b, and Hans D. Hochheimer^c

^a High Pressure Physics Division, Bhabha Atomic Research Center, Mumbai 400085, India

^b Department of Chemistry, Colorado State University, Fort Collins, CO 80523, USA

^c Department of Physics, Colorado State University, Fort Collins, CO 80523, USA

Reprint requests to Prof. Dr. Hans D. Hochheimer. E-mail: dieter@lamar.colostate.edu

Z. Naturforsch. **2008**, *63b*, 661–667; received November 26, 2007

Dedicated to Professor Gérard Demazeau on the occasion of his 65th birthday

Results of a high-pressure angle dispersive X-ray diffraction and electrical resistance study on quasi one-dimensional BaVS₃ are reported. They show that no structural transition occurs up to 26 GPa. However, there is evidence of gradual disordering indicated by the broadening of the diffraction lines. *p*-*V* data fitted to a Birch-Murnaghan equation of state yields a value of the room-temperature, ambient-pressure bulk modulus of 77.3 GPa with a pressure derivative of 4.03. It is proposed that under compression structural phase transitions resulting from static displacements of V ions that are observed at low temperature are suppressed. Instead, a partial “polymerization” of V ions that is dynamic in nature and allows enhanced hopping conduction, starts near 3 GPa and saturates above 15 GPa.

Key words: High Pressure, Low-dimensional Materials, X-Ray Diffraction, Phase Transitions, Transport Measurements

Introduction

Many materials with *d/f* electrons exhibit a wide variety of structural and electronic transitions depending on the dimensionality of the structure, band filling, band width, and the extent of electron-electron correlation and electron-phonon interaction. Transition metal compounds, especially chalcogenides, exhibit a rich variety of phenomena due to a gradual delocalization of electrons in the crystal field split *d* levels (*t*_{2g} and *e*_g) or a change in their occupation number by spontaneous structural distortions or external perturbations. The ternary vanadium sulfide (Ba²⁺V⁴⁺S₃²⁻) is such an example, which upon lowering of the temperature shows three electronically driven structural transitions with special features [1]. At ambient conditions the compound has a “bad-metal” character with a poor, almost isotropic conductivity [2]. It crystallizes in a hexagonal structure (*a* = 6.728, *c* = 5.626 Å; space group *P6₃/mmc* with *Z* = 2) [3]. The structure consists of chains of face sharing S₆ octahedra running along the *c* axis. The Ba²⁺ ions are inside pockets formed by twelve sulfur atoms located between the three well-separated S₆ chains. The active V⁴⁺ ion with an elec-

tronic configuration 3*d*¹ (*S* = 1/2) is located at the center of the sulfur octahedron and forms linear chains along the *c* axis. Thus, the hexagonal BaVS₃ has a quasi one-dimensional structure [4]. The behavior of the single remnant *d* electron of the V ion, modulated by the distortion of the sulfur octahedron, essentially determines the structural and electronic properties of the material. For the S₆ octahedra to be distortion free, the *c/a* ratio should be 0.817 at ambient conditions [5]. The observed value of the *c/a* ratio is, however, 0.836 implying a trigonal distortion of the S₆ octahedra. This results in a further splitting of the *t*_{2g} level of the 3*d*¹ V atomic levels into a non-degenerated *d*_{z²} and doubly degenerated *e*(*t*_{2g}) levels (the nomenclature of Mihaly *et al.* [2] is followed throughout the paper to avoid some confusion that exists in literature). They are directed along the *c* axis and in the *ab* plane, respectively, with the *e*(*t*_{2g}) levels lower in energy. The intra-chain V–V distance (2.805 Å), though larger than the value in metallic vanadium (2.61 Å), is still less than the empirical critical separation for the delocalization of *d* electrons of sulfides, whereas the inter-chain V–V distance (6.72 Å) is far larger than this critical separation. Thus the *d*_{z²} and *e*(*t*_{2g}) levels are expected to evolve

into narrow and quasi-localized bands, respectively. In agreement with these expected features, the results of angle-resolved photoemission spectroscopy measurements [6] and band structure calculations [7] confirm that one-dimensional narrow bands coexist along with quasi-localized levels close to the Fermi energy. As the unit cell contains two molecules, the two available electrons are distributed between lower $e(t_{2g})$ quasi-localized bands and the d_{z^2} band making it half filled. This makes the structure amenable to the Peierls instability. The small anisotropy and the “bad-metal” character is a consequence of the reduction of the influence of the d_{z^2} band through a combination of $d_{z^2} - e(t_{2g})$ scattering and hybridization with sulfur bands and is consistent with the measured coherence length ($\sim 9.7'$) that is of the order of the lattice parameters [6].

The ambient hexagonal structure exhibits dynamic disorder of the V⁴⁺ ions as revealed in its anisotropic temperature factor [8]. This $3d^1$ system undergoes three electronically driven structural phase transitions near temperatures of 240 K (T_S), 70 K (T_{MI}), and 30 K (T_X), but all the phases have pseudo-hexagonal symmetry. Though the measured volume change from 300 to 5 K is only $\sim 1.5\%$ [9], the variation of the c/a ratio is quite unusual; it has a maximum close to T_S and a minimum close to T_{MI} , implying that the fine tuning of the relative positions of the d_{z^2} and $e(t_{2g})$ bands *via* the spontaneous distortions drives these transitions. At T_S , the structural transition is to an orthorhombic (pseudo-hexagonal) phase. It removes the dynamic disorder of the V ions and freezes them into a uniform zigzag chain, resulting in an increase of the V–V distance (2.808 Å at 300 K to 2.845 Å at 100 K). In this phase, one-dimensional structural fluctuations develop with a critical wave vector $q_c = 0.5 c^*$ due to the instability of the electron gas confined along the c axis. These structural fluctuations are detectable from 170 K downward using single crystal X-ray [10] diffraction. The condensation of these fluctuations leads to the I-M transition at 80 K and results in a monoclinic phase (SG: Im) with a doubled c axis (of both orthorhombic and hexagonal pseudo cells). This structure has four inequivalent V ions resulting from the stabilization of two out of phase modulations of the d_{z^2} and $e(t_{2g})$ orbitals [11]. However, susceptibility measurements do not show any sign of long-range magnetic order, that may inhibit hopping conduction, and its absence continues down to a subsequent transition at 30 K (T_X) [2]. This transition at $T_X = 30$ K is accompanied by magnetic ordering and is seen as an anomaly in the resis-

tance [12], an anisotropy in the susceptibility [13], and an incommensurate magnetic order detected by neutron [14] and NMR [15] measurements.

Thus, even though the reduction in volume resulting from lowering the temperature is small, the spontaneous distortion of the octahedra results in condensation of structural and electronic fluctuations in this material.

Compression is expected to have a profound effect on this material by favoring a more three-dimensional structure, by inhibiting charge disproportionation [9], by altering the relative positions, as well as the width and occupancy of the bands, and the electron-electron and electron-phonon interaction.

Electrical resistance measurements at low temperature and high pressure have revealed that the metallic nature of the compound is enhanced, and the T_{MI} transition is suppressed at an average rate of dT_{MI}/dp 0.34 K/GPa [16]. Above a critical pressure of 2.0 GPa, the metallic phase with mysterious magnetic properties extends over the whole temperature range [17]. However, no details of structural evolution are known. Here we report the results of structural and electrical resistance measurements at high pressure at ambient temperature carried out to investigate the structural evolution with pressure at room temperature.

Experimental Section

BaVS₃ was prepared by the stoichiometric combination of elemental Ba, V, and S in a two-step reaction. In the first step Ba, V, and S in stoichiometric proportion were loaded in a quartz ampoule inside a N₂-filled glove box. The ampoule was then sealed under vacuum and placed in a furnace and was ramped to 600 °C at a rate of 5 °C h⁻¹. The temperature was held constant at 600 °C for 48 h, and then the furnace was switched off. The blackish product obtained was ground to a fine powder in an agate mortar and characterized by X-ray diffraction (XRD). The XRD indicated the formation of a mixture of products including binaries such as BaS, V₂S₃ along with BaVS₃. In the second step this powder was again loaded into a quartz ampoule inside the N₂-filled glove box, flame sealed, and held at a constant temperature (750 °C) for 48 h. The furnace was then switched off, and the sample allowed to cool to ambient temperature. The black product was pure BaVS₃ as indicated by XRD.

The angle-dispersive X-ray diffraction (ADXRD) measurements were carried out at the X-ray diffraction beam line at the synchrotron source at Trieste, Italy (Elettra). The X-rays were monochromatized by a double silicon crystal monochromator and the beam collimated to 80 μm diameter employing tungsten pinholes. A 345 mm image plate

(IP) area detector from Mar Research was used for recording the diffraction patterns with 100 μm spatial resolution. The X-ray wavelength (0.6704 \AA) and sample to IP distance (218.8 mm) was calibrated by collecting ADXRD data for silicon and LaB₆. Fine particles of the sample were loaded into a hardened stainless steel gasket hole of 100 μm diameter along with silver as internal pressure marker. A 4:1 methanol-ethanol mixture was used as the pressure-transmitting medium. Prior to loading the sample, the cell with an empty gasket was fixed on a computer-controlled X-Y-Z stage and aligned in the X-ray beam. The data were collected with a typical exposure time of 15 to 30 min for each pressure point depending on the beam intensity. Two-dimensional data obtained as described above were converted to standard one-dimensional patterns using FIT2D software [18]. X-Ray measurements were carried out up to pressures of 27 GPa.

A clamp-type diamond anvil cell with diamond anvils of a culet size of 400 μm was used for the measurements of the electrical resistance. A stainless steel gasket with a 400 μm hole fixed to one of the anvils has been filled with Mylar impregnated alumina (Al₂O₃) powder (0.05 μm grain size) and then been pre-compacted. It serves as insulation and pressure medium with a reduced pressure gradient as compared to the case where only alumina is used. Two 20 μm stainless steel wires centered on the other anvil serve as leads for quasi-four probe measurements. The part of the wires over the anvil face is flattened using a tungsten carbide pin to avoid the shifting of the wires upon pressure increase. Fine powder of ruby is filled between the wires and is used as pressure calibrant. In addition, it ensures that the wires do not shorten when the pressure is increased. The sample in the form of a thin plate is placed in such a way that it covers the wires. The measurements are restricted to a small segment of the sample (40 μm length) in the center of the diamond. After each pressure increase the resistance between the leads and the gasket is measured before the start of the electrical measurement to ensure that there is no shortening of the leads with the gasket. Full details are given elsewhere [19].

Results and Discussion

The evolution of the diffraction patterns with pressures up to 26 GPa is shown in Fig. 1. Above 3 GPa, the diffraction lines broaden with a concomitant increase in background leading to the disappearance of few weak lines. The evolution of the diffraction patterns with pressure indicates that a pressure-induced disorder occurs in the material. Fig. 2, where the full width at half maximum (FWHM) of the strongest [101] reflection is plotted, illustrates this. The FWHM of this line is not affected by an orthorhombic distortion. It ex-

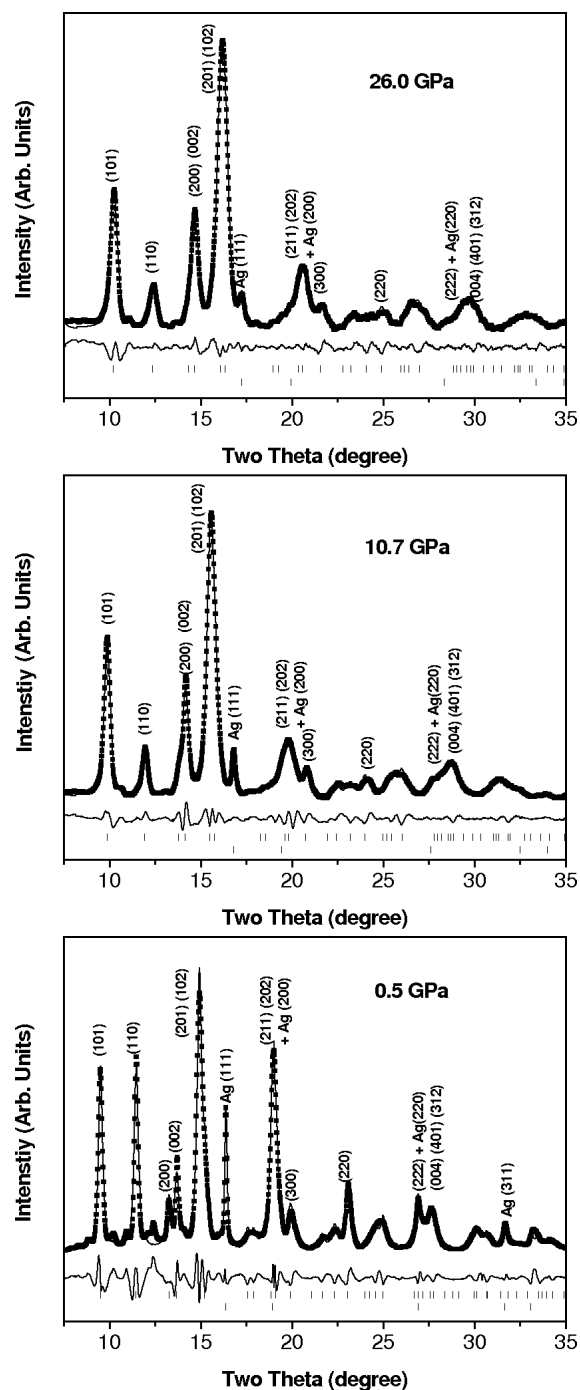


Fig. 1. Pressure evolution of the diffraction patterns at ambient temperature up to 26 GPa. The patterns have been Lebaill-fitted using the GSAS software.

hibits a minimum near 3 GPa and increases fast above 5 GPa. Since the increase in half width starts well be-

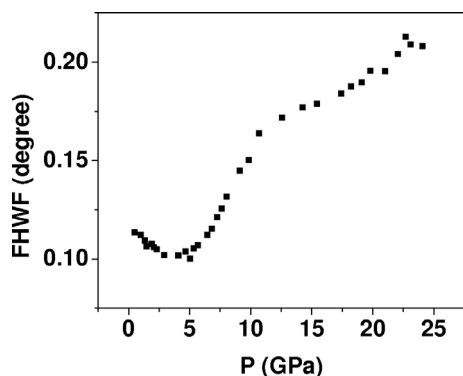


Fig. 2. Pressure dependence of the full width at half maximum (FWHM) of the [101] reflection.

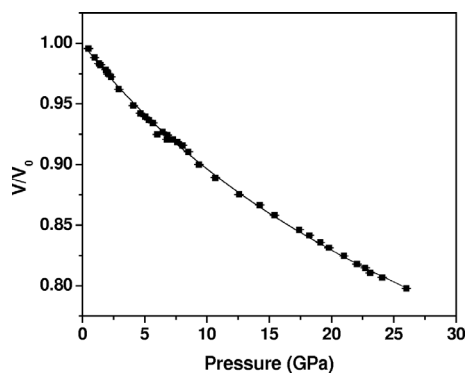


Fig. 3. Pressure dependence of V/V_0 .

low the solidification of the methanol-ethanol mixture, it is clear that it is an intrinsic effect. Up to the highest pressure the patterns can be indexed using the hexagonal cell. In order to obtain the lattice parameters and p - V data, the whole pattern was profile-fitted using GSAS [20]. To exclude the possibility of a structural transition to a phase similar to the orthorhombic low-temperature phase as the reason for the line broadening, full-pattern profile refinements were also carried out using the orthorhombic super cell ($a_o = a_h$, $b_o = b_h/\sqrt{3}$, $c_o = c_h$). It was observed that the dimensions of the orthorhombic cell correspond indeed within the experimental error with that of the hexagonal cell with the above relation satisfied. This is in contrast to the fact that as temperature is lowered, the orthorhombic splitting [$a_o - b_o/\sqrt{3}$] increases from zero at 250 K to 0.13 at 80 K within a volume reduction of 1.5% [8]. Since the volume reduction in the current measurements is about 20% (at 25 GPa), had there been a transition to an orthorhombic phase, the above relation would have broken. Since this does not happen, it may

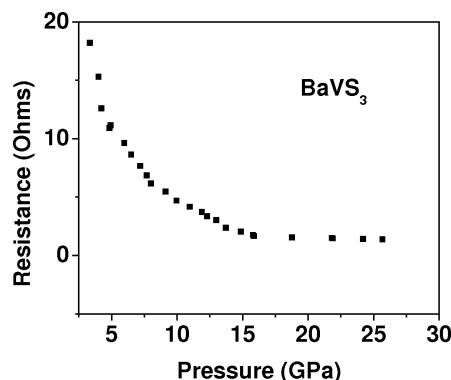


Fig. 4. Pressure dependence of the electrical resistance.

be concluded that there is no structural transition to an orthorhombic phase. Moreover, the hexagonal cell gives an excellent fit over the entire pressure region of the current measurements. The possible reasons for not observing the expected transition and the occurrence of disorder are discussed in the following section.

The p - V curve is smooth in the pressure region of the present measurements (Fig. 3). The bulk modulus and its pressure derivative obtained by fitting the p - V data to the Birch Murnaghan (B-M) equation of state [21] have values of 73.3 GPa and 4.03, respectively.

The results of the electrical resistance measurements are shown in Fig. 4. It shows a gradual increase in conductivity without any discontinuous change consistent with earlier low-temperature, high-pressure measurements [16]. It can also be seen that the resistance does not vary much above 15 GPa.

It is important to point out that the insulating phase below 70 K is caused by the minor distortion of the orthorhombic phase resulting from a tetramerization of the V^{4+} zigzag chain [11]. Thus, the suppression of the insulating phase may indicate that a structural transition to an orthorhombic phase does not occur when high pressure is applied. The fact that the resistance, R , decreases may be due to the broadening of the d_{z^2} band or $d_{z^2} - e(t_{2g})$ decoupling, at least in part. However, this needs to be confirmed by band-structure calculations at high pressure. Another concurrent mechanism, probably a more dominant one, may be the enhanced hopping of carriers due to partial dynamic polymerization as discussed later.

The variation of the cla ratio displayed in Fig. 5 shows some interesting features. It is constant up to 2 GPa and then increases to a maximum of 0.844 above 7 GPa. There is a broad minimum near 12 GPa.

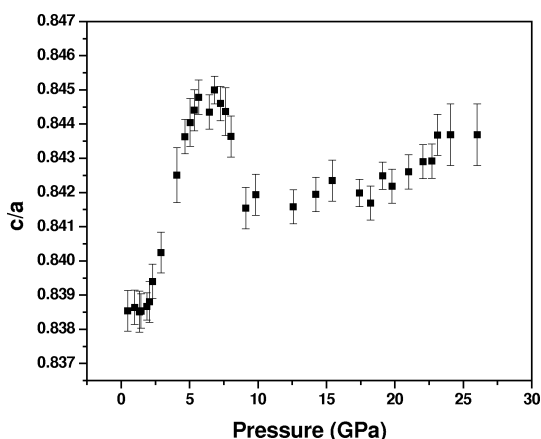


Fig. 5. Pressure dependence of the c/a ratio.

Since the c/a ratio reflects directly the distortion of the S octahedra, it implies that the material has a different structural evolution under pressure as compared to that due to the temperature variation. The c/a value at which the hexagonal to orthorhombic (H-O) structural transition occurs at low temperature (0.839) is reached at 3 GPa. The corresponding volume compression is 2.5% compared to the 1.5% reduction at low temperature. Thus, the axial variation with volume resulting from the application of high pressure and lowering of the temperature is also different.

In the following we examine how the absence of a structural transition is compatible with the structural disorder that is observed.

One important consequence of the one-dimensional structure and the fact that the V^{4+} ions are in a frustrated trigonal lattice in the ab plane is the strong competition between disorder and charge ordering, which leads to the formation of stripped phases in several materials with highly correlated electrons. Thus structural disorder under pressure in this material is not surprising.

The anisotropy of the temperature factor is due to large amplitude vibrations of V^{4+} ions in the ab plane of the hexagonal phase resulting in a larger V–V distance and a dynamical distortion of the V^{4+} substructure [8]. Interestingly, the V–V intrachain distance at low temperatures in the orthorhombic phase remains at 2.84 Å (larger than the 2.80 Å in the hexagonal phase) independent of the orthorhombic distortion. This may be another reason why a transition to the orthorhombic phase is not favored when the volume is reduced. It may be noted that the c/a ratio does not vary much with

pressure until the disorder sets in. If this scenario under pressure is correct, then the introduction of disorder in the V^{4+} ion positions should inhibit structural transitions. In fact, our assumption is supported by the observation that in the slightly disordered $BaV_{0.98}Nb_{0.02}S_3$, all the transitions seen in $BaVS_3$ are suppressed [22].

Apart from the subtle distortion, the temperature induced H-O transition is not reflected in any other physical property except in the electrical resistance, R , where it is seen as a small decrease of the slope of the resistance *versus* temperature curve. The transition shifts to higher temperatures with pressure [5, 16]. If this feature in R is taken as the indicator of the H-O transition, then under pressure, this transition should occur at 300 K near 1.8 GPa [5, 16]. The fact that in our measurement the diffraction lines get sharper up to 3 GPa excludes the possibility of any structural distortion in the above pressure region; *i. e.* it is reasonable to conclude that the orthorhombic phase transition is suppressed under pressure. Though no structural study has been done at high pressure, there are reports of optical [16] and magnetoresistance measurements [17]. These indicate a pressure shift of the M-I transition to lower temperatures [16] and the disappearance of the M-I transition above 2.3 GPa [12]. It may be noted that these measurements also do not show any features associated with the H-O transition.

An interesting aspect of the temperature-induced structural transition seen in Raman investigations in $BaVS_3$ is that it is solely dependent on the V ion arrangement [23]. It is observed that the modes involving the displacement of the S^{2-} and Ba^2 ions do not show any discontinuity across the phase transitions. Apart from a structural transition, there are, however, other possible explanations how the V^{4+} ions can lose their long range order. For example, the removal of the dynamic disorder of the V^{4+} ions by random freezing, or the creation a new type of dynamic disorder due to partial clustering (the general expression “polymerization” used subsequently refers to dimerization and/or tetramerization). It is interesting that the minimum of the half width occurs near the pressure region above which earlier low-temperature, high-pressure measurements have identified an exotic metallic phase, in which the orthorhombic and monoclinic phase transitions are possibly suppressed [16, 17]. Examination of the current measurements in the above context is again consistent with the conclusion that the H-O transition is suppressed at high pressure.

The shifting of the M-I transition to lower temperature and its ultimate suppression above 2.0 GPa [12] gives the clue to the possible origin of the high-pressure behavior of BaVS₃. This implies that the static “polymerization” of the V⁴⁺ ions that causes the low-temperature phase to be insulating [11] do not occur under pressure. However, a polymerization under pressure, if it is partial and dynamic, can retain the short-range order while reducing the long-range order and account for all the features exhibited by BaVS₃. Such a polymerization is implied in the recently reported magnetic behavior at high pressure [17] that shows quenching of the magnetic moment. CuIr₂S₄ is an example of a material with an insulating phase resulting from the polymerization (dimerization) of Ir ions at low temperature [24] and behaves in a similar way at high pressure [25]. In this material, under X-ray irradiation [26] and under compression above 12 GPa [25], the insulating distorted phase transforms into a conducting phase in which short-range order is restored. This results in a higher pseudo-symmetric phase (pseudo-tetragonal phase under X-ray irradiation and a less distorted orthorhombic phase under pressures above 12 GPa) with reduced long range order. Such a dynamic disorder in BaVS₃ (instead of static ordering that results in the orthorhombic phase) due to partial polymerization will yield a conducting disordered phase while retaining the over-

all hexagonal symmetry. This is because in this material, as in CuIr₂S₄, the hopping conduction mechanism is the perceived reason for the nearly isotropic behavior of the electrical resistance in spite of the clearly one-dimensional feature of the crystal structure. If the conduction mechanism is predominantly of the hopping type, then increased conductivity needs an increased number of available hopping sites. A partial polymerization resulting in an increase in equivalent sites due to its dynamic nature satisfies this requirement. Such a partial polymerization will inhibit long range ordering. There is a small difference in the behavior of BaVS₃ and CuIr₂S₄. In CuIr₂S₄, when high pressure is applied, the resistance, *R*, increases initially due to a structural distortion and decreases only after disordering occurs [25]. In BaVS₃ the resistance does not increase under pressure, because there is no static structural distortion at high pressure. CuIr₂Se₂ is probably another material, which behaves in the same way [27]. For this material, the X-ray diffraction pattern at high pressure indicates a loss of long range order. However, no resistance measurements at high pressure covering the same pressure region are available to confirm whether its high-pressure phase is also a more conducting phase.

Thus under pressure, the V ions in BaVS₃ undergo partial polymerization which is dynamic in nature. It starts near 3 GPa and saturates above 15 GPa.

-
- [1] P. Fazekas, K. Penc, K. Radnoczi, N. Barisic, H. Berger, L. Forro, S. Mitrovic, A. Gauzzi, L. Demko, I. Kezsmarki, G. Mihaly, *J. Mag. and Mag. Mat.* **2007**, *310*, 928, and refs. therein.
- [2] G. Mihaly, I. Kezsmarki, F. Zamborszky, M. Miljak, K. Penc, P. Fazekas, H. Berger, L. Forro, *Phys. Rev.* **2000**, *B61*, R7831.
- [3] R. A. Gardener, M. Vlasse, A. Wold, *Acta Crystallogr.* **1968**, *B25*, 781.
- [4] Z. V. Popovic, G. Mihaly, I. Kezsmarki, H. Berger, L. Forro, V. V. Moshchalkov, *Phys. Rev.* **2002**, *B65*, 132301.
- [5] T. Graft, D. Mandrus, J. M. Lawrence, J. D. Thompson, P. C. Canfield, *Phys. Rev.* **1995**, *B51*, 2037.
- [6] S. Mitrovic, P. Fazekas, C. Sondergaard, D. Ariosa, N. Barisic, H. Berger, D. Cloetta, L. Forro, H. Hochst, I. Kupcic, D. Pavuna, G. Margaritondo, *Phys. Rev.* **2007**, *B75*, 153103.
- [7] F. Lechermann, S. Biermann, A. Georges, *Phys. Rev. Lett.* **2005**, *94*, 166402; X. Jiang, G. Y. Guo, *Phys. Rev.* **2004**, *B70*, 035110.
- [8] F. Sayetat, M. Ghedira, J. Chenavas, M. Marezio, *J. Phys. C: Solid State Phys.* **1982**, *15*, 1627.
- [9] M. Ghedira, M. Anne, J. Chenavas, M. Marezio, F. Sayetat, *J. Phys C: Solid State Phys.* **1986**, *19*, 6489.
- [10] S. Fagot, P. Fourt-Leylekian, S. Ravy, J. P. Pouget, H. Berger, *Phys. Rev. Lett.* **2003**, *90*, 196401.
- [11] S. Fagot, P. Fourt-Leylekian, S. Ravy, J. P. Pouget, E. Lorenzo, Y. Joly, M. Greenblatt, M. V. Lobanov, G. Popov, *Phys. Rev.* **2006**, *B73*, 033102.
- [12] L. Forro, R. Gaal, H. Berger, P. Fazekas, K. Penc, I. Kezsmarki, G. Mihaly, *Phys. Rev. Lett.* **2000**, *85*, 1938.
- [13] M. Takano, H. Kosugi, N. Nakanishi, M. Shimada, T. Wada, M. Koizumi, *J. Phys. Soc. Japan* **1977**, *43*, 1101.
- [14] H. Nakamura, T. Yamasaki, S. Giri, H. Imai, M. Shiga, K. Kojima, M. Nishi, K. Kakuai, N. Metoki, *J. Phys. Soc. Japan* **2000**, *69*, 2763; H. Nakamura, H. Tanahashi, H. Imai, M. Shiga, K. Kojima, K. Kakuai, M. Nishi, *J. Phys. Chem. Solids* **1999**, *60*, 1137.

- [15] H. Nakamura, H. Imai, M. Shiga, *Phys. Rev. Lett.* **1997**, *79*, 3779; H. Nishihara, M. Takano, *J. Phys. Soc. Japan* **1981**, *50*, 426.
- [16] I. Kezsmarki, G. Mihaly, R. Gaal, N. Barisic, H. Berger, L. Forro, C. C. Homes, L. Mihaly, *Phys. Rev.* **2005**, *B71*, 193103.
- [17] P. Fazekas, N. Barisic, I. Kezsmarki, L. Demko, H. Berger, L. Forro, G. Mihaly, *Phys. Rev.* **2007**, *B75*, 035128.
- [18] A. P. Hammersley, S. O. Svensson, M. Hanfland, A. N. Fitch, D. Hausermann, *High Press. Res.* **1996**, *14*, 235.
- [19] A. B. Garg, V. Vijayakumar, B. K. Godwal, *Rev. Sci. Instrum.* **2004**, *75*, 2475.
- [20] A. C. Larson, R. B. van Dreele, GSAS: General Structure Analysis System, Rep. LAUR 86-748, Los Alamos National Laboratory, Los Alamos, NM (USA) **2000**.
- [21] F. Birch, *Phys. Rev.* **1947**, *71*, 809.
- [22] P. Foury-Leylekian, S. Fagot, S. Ravy, J. P. Pouget, G. Popov, M. V. Lobanov, M. Greenblatt, *Physica* **2005**, *B359–361*, 1225.
- [23] Z. P. Popvic, G. Mihaly, I. Kezsmarki, H. Berger, L. Forro, V. V. Moshchalkov, *Phys. Rev.* **2002**, *B65*, 132301.
- [24] P. G. Radaelli, Y. Horibe, M. J. Gutmann, H. Ishibashi, C. H. Chen, R. M. Ibberson, Y. Koyama, Y. S. Hor, V. Kiryukhin, S. W. Cheong, *Nature* **2002**, *416*, 155.
- [25] A. B. Garg, V. Vijayakumar, B. K. Godwal, A. Choudhury, H. D. Hochheimer, *Solid State Commun.* **2007**, *142*, 369.
- [26] H. Ishibashi, T. Y. Koo, Y. S. Hor, A. Borissov, P. G. Radaelli, Y. Horibe, S. W. Cheong, V. Kiryukhin, *Phys. Rev.* **2002**, *B66*, 144424; T. Furubayashi, H. Suzuki, T. Matsumoto, S. Nagata, *Solid State Commun.* **2003**, *126*, 617.
- [27] J. Tang, T. Kikekawa, J. Z. Hu, J. F. Shu, H. K. Mao, T. Furubayashi, A. Matsushita, T. Matsumoto, S. Nagata, *Proceedings of the Int. Conf. On High Pressure Science and Technology (AIRAPT-XV)*, (Eds.: M. H. Manghnani, W. J. Nellis, M. F. Nicol), Universities Press, Hyderabad (India) **2000**, p. 506.